MODELING INSPECTABILITY FOR AN AUTOMATED EDDY CURRENT MEASUREMENT SYSTEM

N. Nakagawa, M. W. Kubovich, and J. C. Moulder

Center for NDE
Iowa State University
Ames, Iowa 50011

INTRODUCTION

We have developed an automated eddy current measurement system in our laboratory for quantitative nondestructive evaluation applications. The heart of the measurement system is a precision impedance analyzer capable of measuring impedance or any impedance related quantity over a wide range in frequency (10^2-10^8 Hz). Data acquisition, processing, analysis, and display is accomplished with a personal computer. Computer-controlled x-y positioning stages permit measurements to be obtained for either one- or two-dimensional scans of the specimen. In this article we describe the measurement system and give examples of its use to measure flaw signals with a uniform-field eddy current probe [1].

We also describe a method for quantitatively assessing the flaw detection capability of this EC measurement station. Although this assessment is specific to our measurement system, the method can, in principle, be applied to any eddy-current probe-instrument combination. The basic task of inspectability analysis is to identify sources of signal variabilities such as noise, and then to estimate the extent of their influence on measurements. A simple analysis of signal-to-noise ratios is not sufficient for a fully quantitative assessment. One accepted measure of inspectability is the so-called probability of detection (POD) [2,3].

In this report, we focus attention on the probability of detecting tight fatigue cracks. To evaluate POD we employ a model-based approach, combining theoretical and experimental methods. Theoretical calculations are used to determine the expected impedance signal due to a tight crack. The variability of impedance measurements is estimated from data accumulated in a series of calibration measurements. These noise measurements were carried out for several EDM notches of known size. One advantage of this model-based approach over a totally empirical approach is that a large number of calibration measurements can be avoided [3,4]. Such measurements can be especially expensive and time-consuming in the case of fatigue cracks,

The POD model we developed provides a measure of inspectability in the form of relative-operating-characteristic (ROC) curves and POD curves, demonstrating the ability of the model to quantitatively assess the crack-detection capability of our EC measurement station.

Review of Progress in Quantitative Nondestructive Evaluation, Vol. 9
Edited by D.O. Thompson and D.E. Chimenti
Plenum Press, New York, 1990

AUTOMATED EDDY CURRENT MEASUREMENT SYSTEM

Data acquisition, processing, analysis, and display are accomplished with a personal computer. Computer-controlled x-y positioning stages permit measurements to be recorded for either one- or two-dimensional scans of specimens. The measurement system is shown schematically in Fig. 1. Not shown in this figure is a manually operated x-y-z translation stage that is used to position the probe over the specimen. During measurements, the probe remains stationary while the specimen, mounted on the computer-controlled x-y translation stage, is scanned under the probe. A step-and-measure mode of operation was employed to scan a 20 x 20 mm area of the specimen at 0.5-mm increments.

Measurements of probe impedance were accomplished with a precision impedance analyzer (HP4194A). For the measurements reported here, the real and imaginary parts of the probe impedance were recorded at 19 discrete frequencies spanning the range of 10 kHz to 10 MHz at each of the 1600 scan points. At each point, a total of 64 individual measurements were averaged to produce the final measurement. Each measurement of a specimen took approximately two hours to complete. Data were stored in 38 individual files: one for each component of the signal (real and imaginary) at each frequency. For the assessment of the performance of this system, measurements were taken on a variety of flaws in 7075 aluminum alloy plates. These included semicircular and rectangular EDM notches, shallow cylindrical (flat-bottom) holes, and one specimen with no flaw present.

The raw data collected as described above were further processed to separate random noise components and signals due to surface tilt and curvature (liftoff signals) from the flaw signals. This process is illustrated in Fig. 2, which shows an example of a measurement at 1 MHz on a cylindrical hole 0.76 mm in diameter and 0.21 mm deep. To subtract the effects of tilt and liftoff, the flaw signal is masked and the remaining data are least-squares fit to a 2nd degree polynomial, producing a smooth surface that is then subtracted from the raw data.

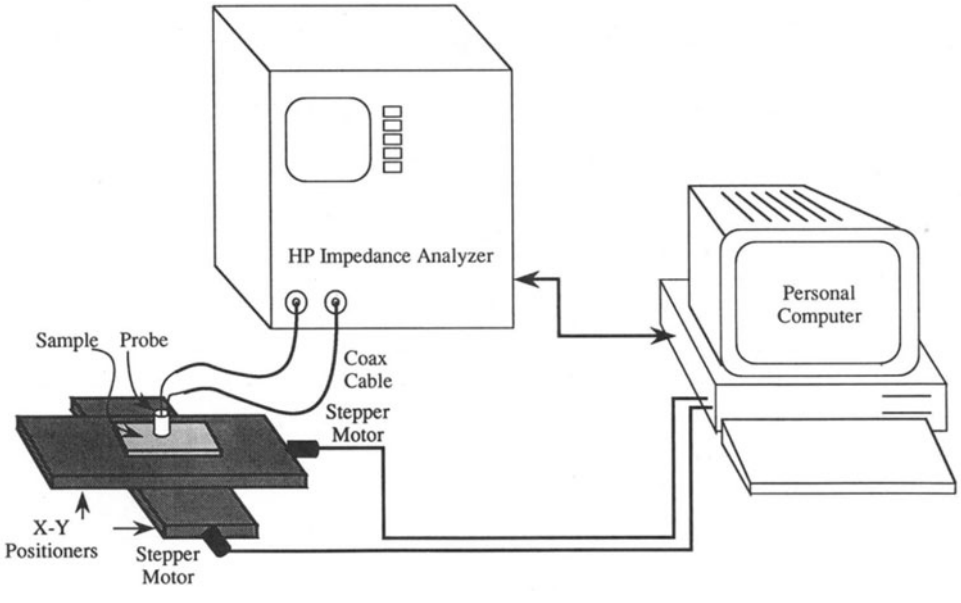

Fig. 1. Schematic diagram of automated eddy current measurement system.

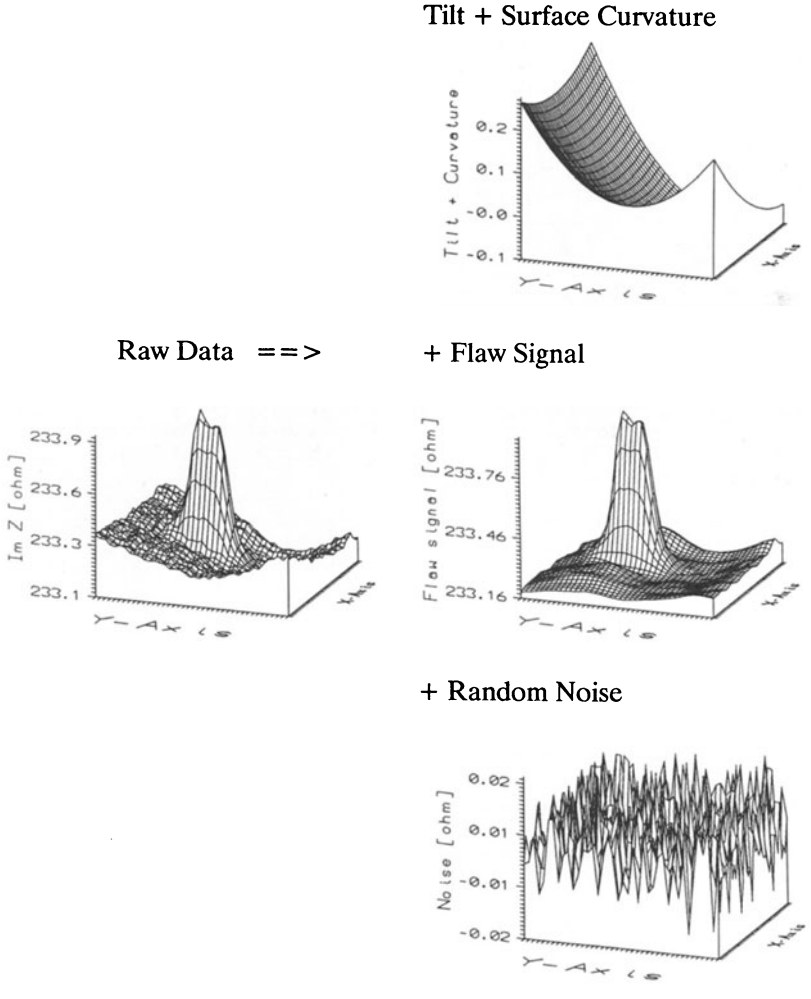

Fig. 2. Signal processing steps used in analyzing eddy current data. Raw data are separated into three components: tilt and surface curvature, random noise, and the flaw signal. Plots are made with respect to the scan plane.

Next, the data are smoothed with a spline-function smoothing routine that is passed over each row and column of data. The smoothed data set is then subtracted from the tilt-corrected data to obtain the random noise present in the measured data. Thus we obtain three components of the signal: flaw impedance, tilt and surface curvature, and random noise. All three components are used in the POD analysis that is described next.

MODELING INSPECTABILITY

Next, we describe the POD model, which gives a quantitative assessment of the fatigue-crack detection capability of our EC measurement station. As described in the introduction, our POD model was built around both theory and experiment. We will briefly discuss the theory and the calibration data used in the model.

Approach

To determine the expected impedance signal we used theoretical results. To model our measurement system we needed predictions for uniform-field-probe signals due to a tightly closed crack. Several methods for calculating flaw impedance in a uniform applied field applicable to various frequency ranges can be found in the literature [5-7]. Here, the crack impedance was evaluated by a combination of these methods for necessary parameter ranges. Namely, the crack was assumed to be of a semi-elliptical shape, and its dimensions were chosen to lie in such a range that the aspect ratio (length/depth) was between 2 and 5, and the crack depth was not less than 10% of the skin depth. The numerical result thus obtained was then approximated by a collection of bicubic spline functions. It was these spline functions that were implemented into the POD code explicitly, thus achieving an efficient numerical procedure.

One problem that arises in calculating flaw signals is that a theoretical prediction must be multiplied by an overall constant (including both magnitude and phase) which remains undetermined theoretically. In our approach, it was set by calibration measurements at each of the chosen frequencies. These calibration measurements were taken with cylindrical pits of known sizes machined on aluminum blocks. The constants were then determined by comparing the measurements with Auld's high-frequency theory.

To formulate the variability of measured impedance Z, we studied the distribution of measured values in the complex plane. Figure 3 shows a typical example of probe impedance distributions. There, the topographical map (1) is a distribution of impedance measurements in the absence of any flaw, while (2) is in the presence of a crack. Distributions such as these lead us to consider that both real and imaginary parts of Z are random variables

$$Z = R + iX. \tag{1}$$

Let the means of R and X be $\bar{r}$ and $\bar{x}$. Because R and X are not stochastically independent, one needs to consider a two-dimensional probability density function $f(r-\bar{r}, x-\bar{x})$. Here, we assumed that the fluctuations follow a two-dimensional Gaussian distribution. Then, the three basic parameters of f can be determined by fitting them to experimental values of $<R^2>-<R>^2$, $<X^2>-<X>^2$, and $<RX>-<R><X>$. In practice, we determined our f using the processed data described in the preceding section. Out of the processed data, we isolated noise components by subtracting the tilt and the smoothed flaw signal from the raw data. We repeated this fitting procedure for various frequencies, using different flaw measurements, including a measurement with a no-flaw sample. We found that the f parameters thus determined varied from flaw to flaw, but that the variations were as small as a few percent.

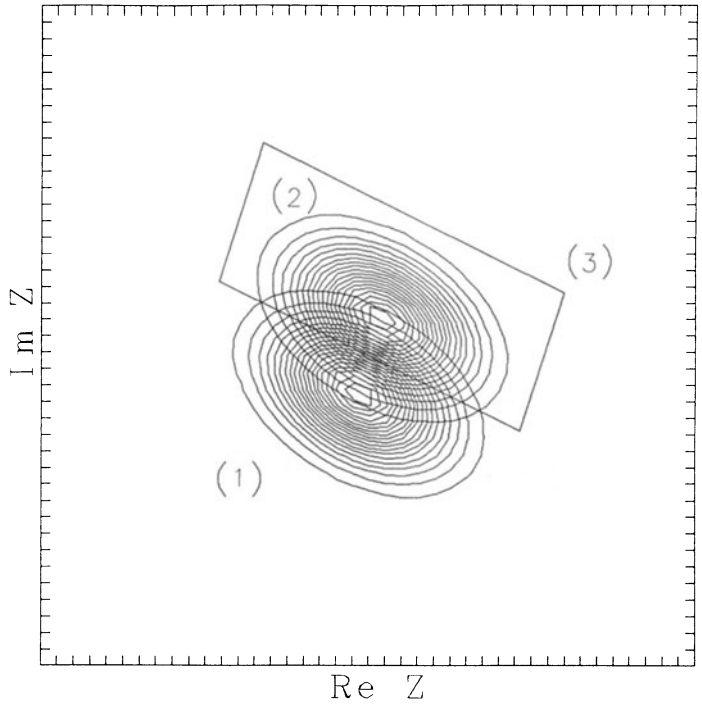

Fig. 3. An example of probe signal distributions in the complex impedance plane: The topographical plot (1) shows a distribution of no-flaw signals, while (2) is an on-flaw signal distribution. Graphically, the shift between (1) and (2) corresponds to a predicted crack impedance. The domain (3) is an example of threshold domains, over which the distributions are integrated to yield PFA and POD.

ROC and POD Curves

In terms of the probability density function f, the distributions (1) and (2) of Fig. 3 can be written as $f(r-r_1, x-x_1)$ and $f(r-r_2, x-x_2)$, where (r_1+ix_1) [resp. (r_2+ix_2)] denotes the average impedance without [with] a crack. These distributions are then integrated over a selected domain D, such as (3) in Fig. 3, yielding probability of false alarm (PFA) and POD, respectively.

There are two traditional ways of expressing inspectability, one in terms of ROC curves, and the other as POD-vs-size plots. The ROC curves are loci in the PFA-POD plane traced by pairs of PFA and POD, which are evaluated for continuously varying threshold boundaries of D while the crack size is kept fixed. In contrast, the POD plots can be obtained by calculating POD as a function of crack size for a fixed threshold value. Our sample ROC results are given in Fig. 4. Also, examples of POD-vs-size plots are given in Fig. 5. The ROC results indicate the basic ability of our EC measurement system to separate crack signals from background noise. The POD plots, on the other hand, are useful in studying its ability to discriminate crack sizes in the vicinity of a critical crack size.

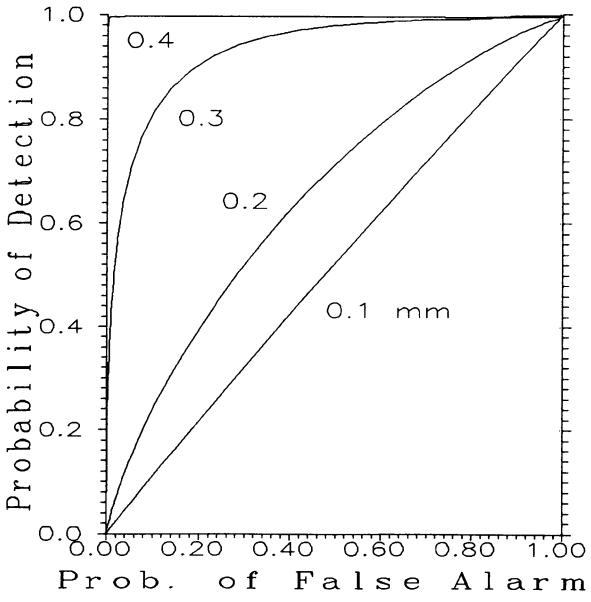

Fig. 4. Predicted relative operating characteristics. Here, the probe is a uniform-field probe, operating at 100 kHz. The specimen is an aluminum block with a flat surface. The crack is assumed to be semi-elliptical, with an aspect ratio of 3. Four cracks of depths 0.1, 0.2, 0.3, and 0.4 mm were studied explicitly.

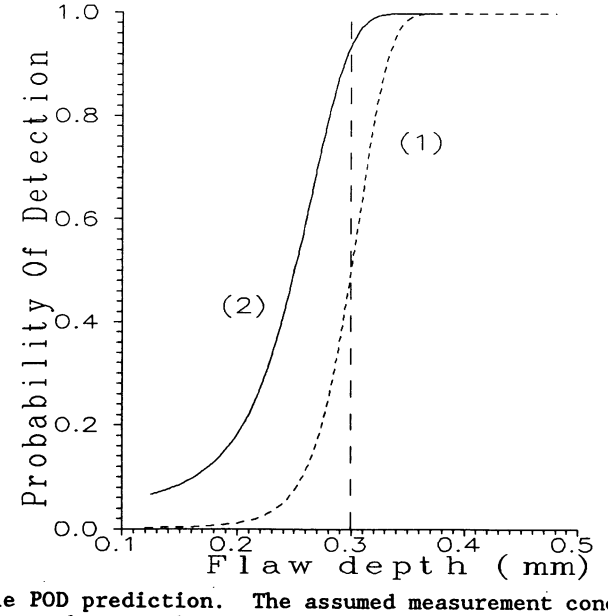

Fig. 5. A sample POD prediction. The assumed measurement condition is similar to the example in Fig. 4, except that the probe frequency is 141 kHz. The dotted curve (1) was obtained by setting the threshold value to 6.5 [$m\Omega$] where the POD of a 0.3-mm crack is 50%. The solid curve (2) is for a threshold of 3.7 [$m\Omega$] where 95% POD is achieved for a 0.3-mm crack.

CONCLUSION

In this report we described an automated EC measurement station, based upon a precision impedance analyzer with computer-controlled data acquisition and analysis. Results presented here demonstrate that this measurement system is suitable for efficiently collecting the precise impedance data needed for quantitative NDE measurements. We also described a method for quantitatively assessing the performance of this system by combining theoretical predictions of flaw signals with empirical characterization of the signal variability. This assessment, embodied in graphs of the relative operating characteristics (ROC) or in plots of probability of detection versus flaw size, demonstrated that measurements with this system are of sufficient quality to allow quantitative studies of the probability of tight-crack detection.

ACKNOWLEDGMENTS

This work was supported by the Center for NDE at Iowa State University, and performed at Ames Laboratory, USDOE. Ames Laboratory is operated for the U.S. Department of Energy by Iowa State University under Contract No. W-7405-ENG-82.

REFERENCES

1. E. Smith, "Uniform interrogating field eddy current technique and its application," in Review of Progress in Quantitative NDE, Vol. 5A, D. O. Thompson and D. E. Chimenti, eds., Plenum, New York (1986); J. C. Moulder, P. J. Shull, and T. E. Capobianco, "Uniform field eddy current probe: experiments and inversion for realistic flaws," in Review of Progress in Quantitative NDE, Vol. 6A, D. O. Thompson and D. E. Chimenti, eds., Plenum, New York (1987); P. J. Shull, T. E. Capobianco, and J. C. Moulder, "Design and characterization of uniform field eddy current probes," in Review of Progress in Quantitative NDE, Vol. 6A, D. O. Thompson and D. E. Chimenti, eds., Plenum, New York (1987).

2. A. J. Bahr, "System analysis of eddy-current measurements," in Review of Progress in Quantitative NDE, Vol. 1, D. O. Thompson and D. E. Chimenti, eds., Plenum, New York (1982); A. J. Bahr and D. W. Cooley, "Analysis and design of eddy-current systems," in Review of Progress in Quantitative NDE, Vol. 2A, D. O. Thompson and D. E. Chimenti, eds., Plenum, New York (1983); J. R. Martinez and A. J. Bahr, "Statistical detection model," in Review of Progress in Quantitative NDE, Vol. 3A, D. O. Thompson and D. E. Chimenti, eds., Plenum, New York (1984).

3. R. E. Beissner, K. A. Bartels, and J. L. Fisher, in Review of Progress in Quantitative NDE, edited by D. O. Thompson and D. E. Chimenti (Plenum Press, New York, 1988), Vol. 7B, pp. 1753-1760.

4. N. Nakagawa and R. E. Beissner, "Probability of tight crack detection," in this volume.

5. T.G. Kincaid, "A theory of eddy current NDE for cracks in nonmagnetic materials," in Review of Progress in Quantitative NDE, Vol. 1, D. O. Thompson and D. E. Chimenti, eds., Plenum, New York (1982).

6. B. A. Auld, F. G. Muennemann, and D. K. Winslow, J. Nondestr. Eval. 2, 1 (1982); B. A. Auld, F. G. Muennemann, and M. Riaziat, "Quantitative Modeling of Flaw Responses in Eddy Current Testing," in Research Techniques in Nondestructive Testing, Vol. 7, R. S. Sharpe, ed., Academic Press, London (1984).

7. N. Nakagawa, in Review of Progress in Quantitative NDE, edited by D. O. Thompson and D. E. Chimenti (Plenum Press, New York, 1989), Vol. 8A, pp. 245-250.